*ГЕОФИЗИЧЕСКИЕ ИССЛЕДОВАНИЯ, 2016, том 17, № 3, с.32-44. DOI: 10.21455/gr2016.3-3*

*УДК 550.344.42, 551.510.535, 537.87*

# THE LOWER IONOSPHERE ELECTROMAGNETIC RESPONSE TO TSUNAMI PROPAGATION

M.S. Solovieva[1], A.A. Rozhnoi[1], S.L. Shalimov[1,2], B.W. Levin[3], G.V. Shevchenko[3], V.B. Gurianov[3]

[1] *Schmidt Institute of Physics of the Earth, Russian Academy of Sciences, Moscow, Russia*
[2] *Space Research Institute, Russian Academy of Sciences, Moscow, Russia*
[3] *Institute of Marine Geology and Geophysics, Far East Branch, Russian Academy of Sciences, Yuzhno-Sakhalinsk, Russia*

**Abstract.** The observations of the very low frequency (VLF) electromagnetic signals at stations in Russia (Petropavlovsk-Kamchatsky and Yuzhno-Sakhalinsk) and Japan (Moshiri) have been used to analyze the response of the lower ionosphere to the tsunamis triggered by the Kuril, 2006, Japan, 2011, and Chile, 2010, earthquakes. A significant decrease in the amplitude (about 10–15 dB) together with phase variations of up to 40 degrees relative to the normal signal level have been found after the earthquakes during the tsunami wave propagation along the path transmitter–receiver. The analysis of the VLF signal was carried out for nighttime observations when the ionosphere is more sensitive to external factors than the sunlit ionosphere. The results of analysis of the VLF observations were compared to the sea-level measurements from Japanese network of GPS buoys situated along Japan coastline for the Japan tsunami and with data from the Deep-ocean Assessments and Reporting of Tsunamis (DART) stations situated in the Pacific Ocean near Hawaiian Islands and offshore Kamchatka for the Chilean tsunami. The analysis of spectral characteristics of VLF variations has shown good coincidence of the frequency maxima with in-situ data of sea-level fluctuations (8–50 min). The results of the work confirm that the detected lower ionosphere perturbations are likely generated by the tsunami-driven internal gravity waves.

**Keywords:** tsunami, sub-ionospheric electromagnetic signals, the lower ionosphere, internal gravity waves.

## Introduction

Ionospheric effects resulted from tsunami waves propagation are sufficiently proved during the last decade. Experimental observations of ionosphere response to tsunami are based on theoretical works about propagation of gravity waves in the atmosphere, published in 70-ies of the last century (see, for example, [*Hines,* 1972; *Najita, Weaver, Yuen,* 1974; *Peltier, Hines,* 1976]). Tsunamis generate internal gravity waves that propagate upward into the atmosphere, where their amplitude increases due to the decrease in air density with the altitude. These waves dissipate and thus cause plasma density perturbations when they reach ionospheric heights. Such perturbations can be registered by GPS satellites as well as by the method of very low frequencies (VLF) ionosperic sounding.

Such perturbations in the ionosphere were discovered for the first time in 2005 [*Artru et al.,* 2005]. Measurements of total electron content (TEC) were performed by the network of GPS stations in Japan and used for analysis of tsunami caused by the Peru earthquake on 23.06.2001. Occhipinti et al. [2006] used the three-dimensional modelling of interaction between ocean, atmosphere, and ionosphere to confirm the tsunamigenic hypothesis of the origin of observed perturbations and reproduced the perturbations in TEC for tsunami caused by the earthquake in 2004 near Sumatra. Such perturbations in TEC were detected also for several other strong tsunamis in the Pacific Ocean [*Galvan et al.,* 2011; *Komjathy et al.,* 2012]. Rolland et al. [2010] compared spectral characteristics of TEC variations with data on sea level fluctuations near Hawaiian Islands and confirmed the hypothesis that GPS data can reveal anomalies related to tsunami.

Makela et al. [2011] used photometrical measurements to analyze tsunami caused by the Japan, 2011, earthquake and discovered variations of glow in the ionosphere. Earlier simulation studies showed that significant modulation of luminous intensity in the line of 630.0 nm can be caused by gravity waves that are generated during tsunami propagation [*Hickey, Schubert, Walterscheid,* 2010]. Results obtained in [*Makela et al.,* 2011] were successfully modelled and reproduced in [*Occhipinti et al.,* 2011], providing an explanation of gravity waves generation from tsunami. Mainly, the ionospheric perturbations are observed in the far field (more than 500 km from the earthquake epicenter) where they are clearly visible, because in this zone are generated the gravity waves caused by tsunami.

The methods and observations described above are related to the response of upper ionosphere, F-zone to the tsunami propagation. As shown, this response is initiated by internal gravity waves penetrating in F-zone. However, before reaching this zone, the gravity waves are propagating through lower ionosphere, where in addition to generating penetrations in ionization they cause changes in chemical composition of thermosphere. It should be noted that perturbations in E-zone of ionosphere caused by tsunamigenic gravity waves were studied both numerically [*Occhipinti, Kherani, Lognonné,* 2008] and theoretically [*Coïsson et al.,* 2011].

One of the few experimental methods that allow to register changes in ionization of lower ionosphere, is a method of VLF sounding. Waves of VLF range (3-30kHz) propagate between the Earth and ionosphere as in spherical waveguide, where the low wall is the Earth and the upper wall is the lower lay of ionosphere. Effective height of signal reflection is usually ~70 km by day, and ~90 km at night. The propagation of VLF signals depends mainly on the reflection height that is determined by the magnitude and gradient of electron density near the atmosphere-ionosphere boundary [*Barr, Jones, Rodger,* 2000]. Modification of ionospheric density causes changes in amplitude and phase of detected VLF signals. Their propagation at distances of thousands and tens of thousands of kilometers gives the opportunity to control the state of upper atmosphere and lower ionosphere within large regions. Thus, although receivers and transmitters are located on the land, it is possible, for example, to track the changes in electron density of lower ionosphere above large territory of the Pacific Ocean. Rozhnoi et al. [2012, 2014] first considered the response of the lower ionosphere to the tsunami propagation.

This paper describes the results of using the method of VLF sounding for monitoring the response of lower ionosphere to tsunamis caused by three earthquakes: the Kuril, 2006, the Japanese, 2011, and the Chilean, 2010.

## Initial data and observational method

The work is based on registration of VLF/LF (~20–40 kHz) at stations located on the territory of Russia in Petropavlovsk-Kamchatsky (PTK) and Yuzhno-Sakhalinsk (YSH), and also on the territory of Japan in Moshiri (MSR). Receivers at the stations simultaneously measure the amplitude (in Db) and phase (in degrees) of the signals with the sampling interval of 20 s from several transmitters located in Japan (JJY, 40 kHz and JJI, 22.2 kHz), Australia (NWC, 19.8 kHz), and on Hawaii (NPM, 21.4 kHz). For the Japanese transmitter JJI is registered only the amplitude, as its incoming signal is not MSK modulated (Minimum Shift Keying), therefore it can't be received by the used equipment.

Data of VLF measurements were compared with data obtained at the deep-water stations DART (Deep-ocean Assessments and Reporting of Tsunamis) disposed by the National Oceanic and Atmospheric Administration of the USA (http://www.ndbc.noaa.gov/dart.shtml) and also at the GPS stations of the Japanese Information Network NOWPHAS (http://www.pari.go.jp/unit/kaisy/nowphas/).

Figure 1 shows the scheme of the studied region with the location of epicenters of two earthquakes with $M$>8: the Japanese, 11.03.2011, earthquake (II in Figures) and the Kuril, 15.11.2006, earthquake (I in Figures); DART and GPS stations, as well as receivers and transmitters. The sensitivity zones of different paths are also shown.

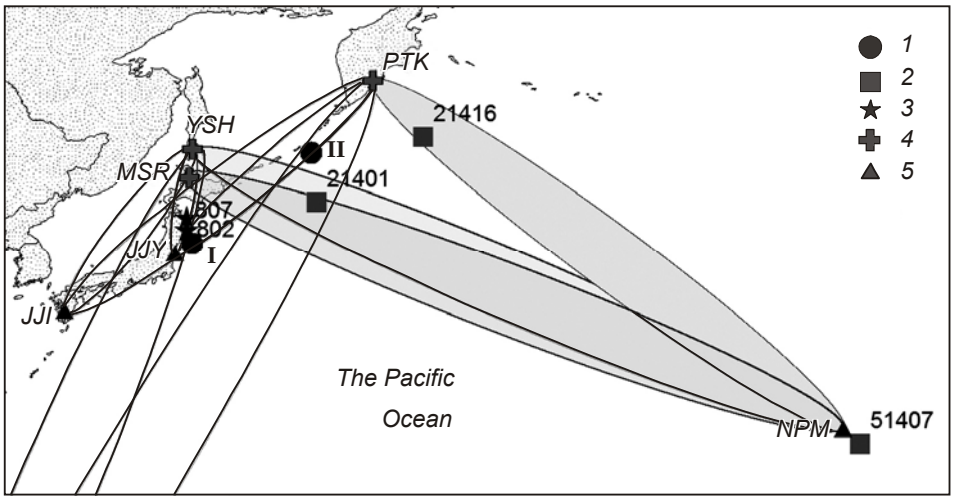


**Fig. 1.** The scheme of the studied region showing the location of (*1*) epicenters of two earthquakes with $M$>8, (*2*) *DART* and (*3*) *GPS* stations with their numbers, as well as (*4*) receivers and (*5*) transmitters. Ellipses with gray filling are zones of sensitivity of paths from NPM transmitter; without filling are from JJY, JJI, and NWC transmitters. For NWC transmitter (19.8 kHz) located in Australia (not shown in the diagram) only part of the sensitivity zone is given (according to the data of USGS/NEIC http://neic.usgs.gov/neis/epic/epic_global.html).

Zones of paths sensitivity correspond to five Fresnel zones (ellipses on the diagram). Coordinates of the projection of the first zone on the earth's surface were calculated by the formula $y=[\lambda^2/4+\lambda x(1-x/D)]^{1/2}$, where $\lambda$ is the wave length; $x$ is a coordinate along the path of signal propagation; and $D$ is the distance between receiver and transmitter. Ellipses with gray filling are zones of sensitivity of paths from transmitter *NPM*, which direction coincides with the direction of tsunami propagation. Other subionospheric paths were used as check paths. Signal was analyzed at night when the ionosphere is more sensitive to external influences. Characteristics of daytime and nighttime ionospheres are substantially different. The state of sunlit ionosphere is solely determined by solar activity. As was mentioned above, the altitude of the daytime ionosphere is significantly lower than the nighttime, due to the formation of sporadic layer caused by solar radiation. During the day in ionosphere is possible the occurrence of sudden ionospheric perturbations caused by X-rays during solar flares on the day-side of the Earth. These perturbations are well-monitored by VLF/LF signals in the form of sudden phase anomalies. Other external influences, magnetic storms, proton flares, electron flows, typhoons, seismic, and volcanic activity (especially on mid- and low-latitude paths), can cause perturbations in the ionosphere and, consequently, in characteristics of subionospheric LF signals only at the night.

## The results of the analysis

### *Kuril tsunami of 15 November, 2006*

The first earthquake selected for the analysis occurred on 15.11.2006 near Simushir island (Kuril Islands) at 11:14 UT ($M_w$=8.3, $h$=34 km). The earthquake caused a tsunami that

was registered by tide-gauges of Tsunami Warning Center [http://wcatwc.arh.noaa.gov/about /tsunamimain.php]. For the analysis of variations of VLF signal after the earthquake, the path NPM - Petropavlovsk-Kamchatsky was selected, since its direction coincides with the direction of tsunami propagation. Station in Yuzhno-Sakhalinsk was established in 2009 and, therefore, was not available at the time of considered earthquake.

The analysis compares the signals propagating along the paths JJY-PTK, JJI-PTK, and NWC-PTK. Figure 2 shows differential values of amplitude and phase of signals at the PTK station during local night on 15.11.2006, defined as difference between current and model signal. The model signal used was the average monthly signal calculated for unperturbed, quiet days in each month.

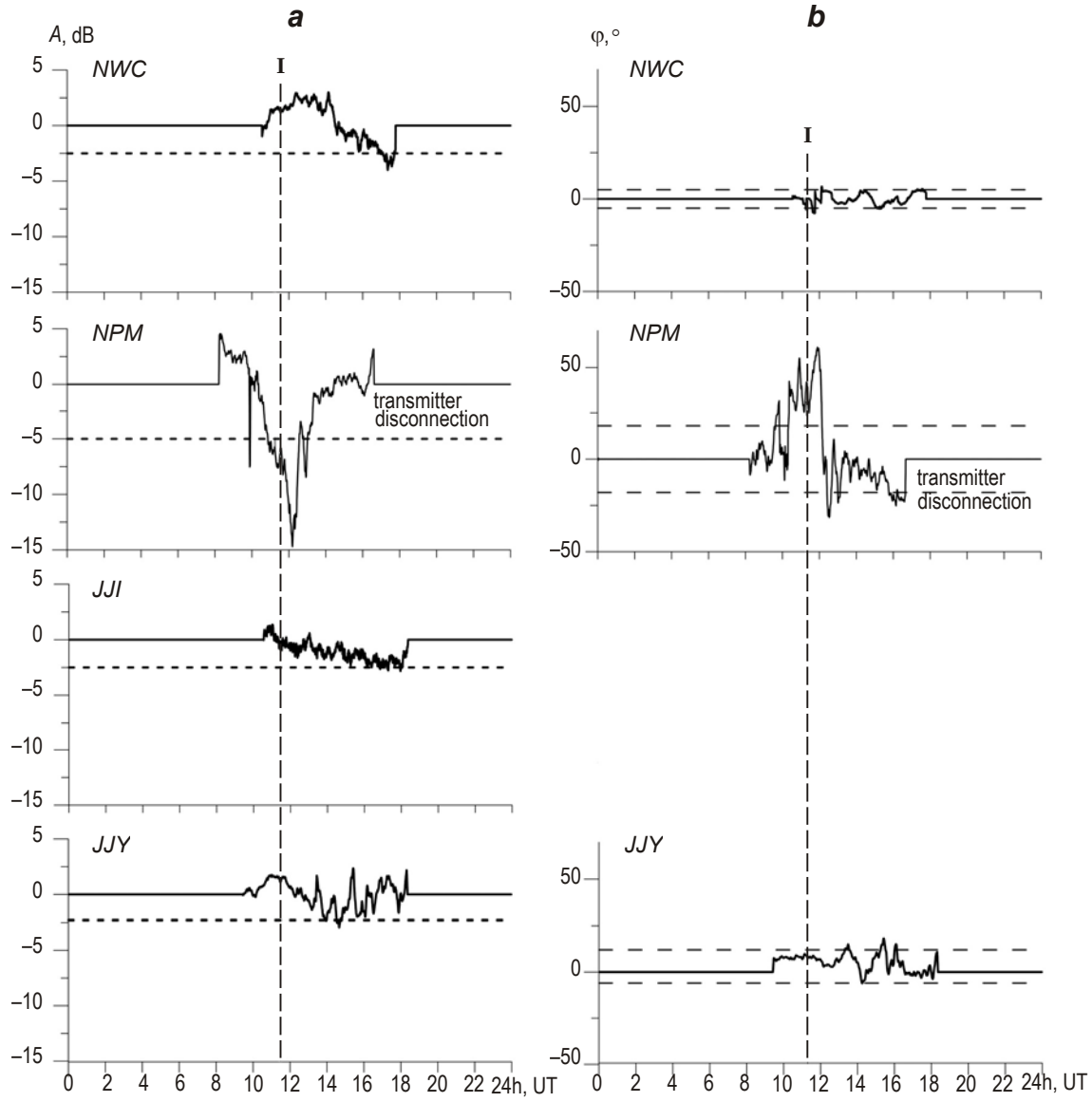


**Fig. 2.** Differential (*a*) amplitudes and (*b*) phases of signals from transmitters NWC (19.8 kHz), NPM (21.4 kHz), JJI (22.2 kHz), and JJY (40.0 kHz) recorded in nighttime on 15.11.2006 at PTK station. Zero lines refer to the daytime; horizontal dashed lines are the average values $-2\sigma$ on (*a*) and average values $\pm 2\sigma$ on (b); vertical dashed line shows the time of the earthquake I on 15.11.2006 near Simushir island.

The night amplitude anomalies of VLF/LF signals caused by different factors (geomagnetic activity, stream of elementary cosmic particles, atmosphere circulation, tsunami, seismic, and volcanic activity, etc.) are always negative due to signal dissipation on ionospheric irregularities, so only negative standard deviations (– 2σ) are plotted in this and further figures for amplitudes

Phase anomalies can be either completely negative (positive) or can have variable signs, so the plots give ±2σ values.

As seen from Fig. 2, differential values of amplitudes and phases of signals from all transmitters during the local night on 15.11.2006 (with the exception of NPM transmitter) are within dispersion boundaries. However, for the NPM transmitter, there is a significant (almost 10 dB below the level of standard deviation) reduction in differential amplitude. Differential phase of the same signal displays visible phase anomalies exceeding the level of 2σ at 40°. The time interval between the moment of the earthquake and maximum of signal anomaly is about 1-1.2 h. It should be noted that a sharp drop in amplitude and increase in phase about in hour before the earthquake are caused by transmitter shutdown. The transmitter also became disconnected approximately in 5 h after the earthquake due to electromagnetic noise in signal records.

Amplitude and phase of the signal from the transmitter NPM, registered on 15.11.2006, were filtered in the range 0.3-15 MHz (period from 1 to 55 min). Wavelet analysis of the filtered signal showed that frequency maximum of its spectrum is in the interval of 8-30 min that corresponds to internal gravity waves (waves with periods longer than 6 min).

*Japanese tsunami of 11 March, 2011*

The earthquake with the magnitude $M_w$=9.0 occurred on 11.03.2011 at 05:46 UT in Japan near Tohoku. According to the NEIC/USGS catalogue, the epicenter of the main shock was located at 38.322°N and 142.369°E; focal depth was 24 km. This earthquake caused the devastating tsunami with wave height of 10-15 m (in some places up to 20 m). Tsunami was recorded by the instruments of Tsunami Warning Center located across all water area of the Pacific Ocean. The tsunami caused severe damage to the North-East coast of Honshu and leaded to thousands of casualties and vast destruction including anthropogenic catastrophe at the Fukushima 1 nuclear power plant.

For the analysis, we used data from the YSH and MSR stations. Direction of tsunami propagation in this case coincided with direction of paths NPM–YSH and NPM–MSR (see Fig. 1). Differential values of amplitude and phase of NPM signal registered on 11.03.2011 by stations YSH and MSR are shown in Fig.3.

Strong negative anomalies of signal amplitude exceeding the level of 2σ for 6-15 dB and positive phase variations up to 40° relative to the 2σ level can be easily traced on the records of both stations. It should be noted that the records from other transmitters (JJY, JJI, and NWC), obtained on the same day, exhibit no noticeable perturbations. Anomalies in Fig.3 are observed during the entire local night (8–16 UT). Maximum of signal anomaly was observed more than 3 h after the earthquake (in the previous case after 1-1.5 h) [*Rozhnoi et al.,* 2012]. The Tohoku earthquake occurred during the evening terminator (transition from day to night) at sharp change of altitude of lower ionosphere boundary, leading to strong perturbations of VLF signal, against which the real beginning of anomaly may be indistinguishable.

Figure 4 (*e* and *f*) shows wavelet-spectra of *NPM* signal (filtered in the range from 1 to 55 min), registered in Moshiri on 11.03.2011 during the local night. Maximum of signal spectrum is in the frequency range of 0.3-2 MHz (or 8-55 min) both for amplitude and phase of the

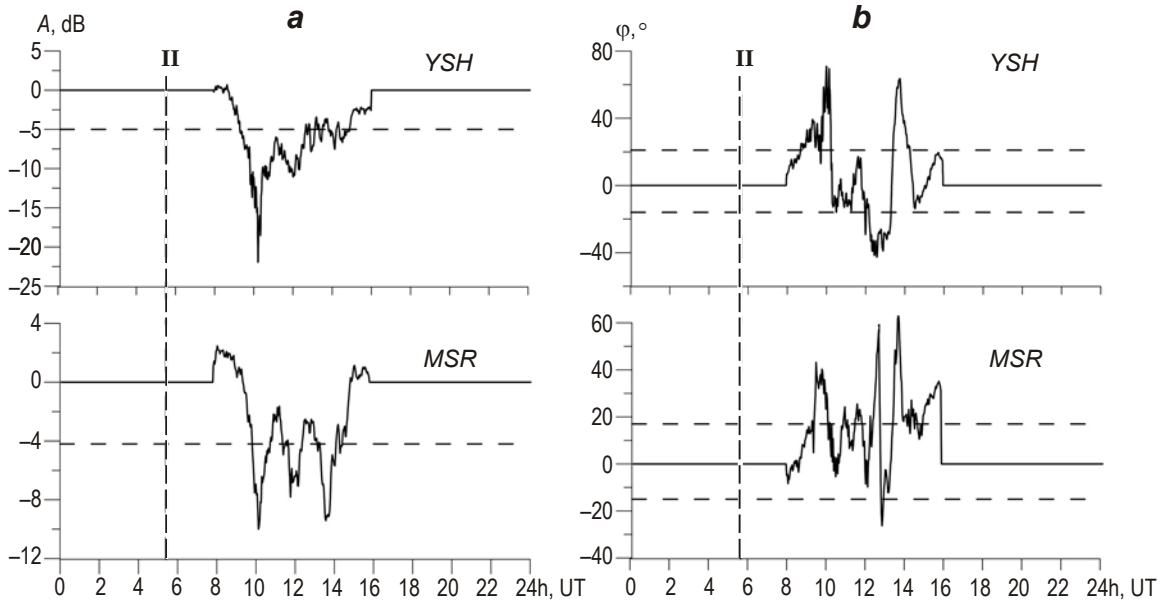


**Fig. 3.** Differential (*a*) amplitudes and (*b*) phases of signals from the NPM transmitter (21.4 kHz), registered by stations in Yuzhno-Sakhalinsk (YSH) and Moshiri (MSR) in nighttime on 11.03.2011. Notations see in Fig.2

signal. Tsunami comes to the buoy 21401 during the evening terminator. Therefore, the interaction of internal gravity waves with ionosphere is not so effective and maximum of VLF anomaly is observed with the delay of about 2 hours after the beginning of local night. It can be seen that gravity waves start to interact with lower ionosphere approximately in 1-1.5 h after the earthquake during the passage of the evening terminator.

Figure 4, *b* shows the arrival times of tsunami wave to the buoy 21401 located inside sensitivity zone of paths NPM–YSH and NPM–MSR at a distance of about ~1000 km from receivers and to the buoy 51407 located near Hawaii. VLF signal remained perturbed all the time of tsunami propagation from Japan to Hawaii. Similar analysis carried out for NPM signal registered at the same time in Yuzhno-Sakhalinsk showed the same results.

Results of VLF signal analysis were compared with spectral characteristics of sea level fluctuations recorded at Japanese GPS stations NOWPHAS. Stations on buoys 802 and 807 (see Fig.1) were selected for comparison as they are located closest to the VLF station in Moshiri. The corresponding wavelet-spectra are presented in Fig.5. On buoy 802, the tsunami wave was registered around 6:00 UT; on buoy 807, around 6:15 UT, i.e. approximately in 15 min (buoy 807) and 30 min (buoy 807) after the earthquake. The maximum of oscillation energy was in the range from 25 to 55 min on the buoy 807, and 15-55 min on the buoy 802; weaker maximums are observed in the range of 8-20 min (buoy 807) and 6-15 (buoy 802).

Thus, spectra of see level fluctuations are in good agreement with spectra of perturbed VLF signal observed after the earthquake. Found periods also correspond with periods of internal gravity waves.

### *Chilean tsunami of 27–28 February, 2010*

Strong earthquake with $M_w$=8.8 occurred on 27.02.2010 at 06:34 UT near the coast of Chili. According to the USGS/NEIC catalogue, the epicenter of the main shock had coordinates 35.846°S and 72.719°W, focal depth was 35 km. The earthquake was followed by a strong tsunami that caused significant destructions along the Chilean coast and was a serious

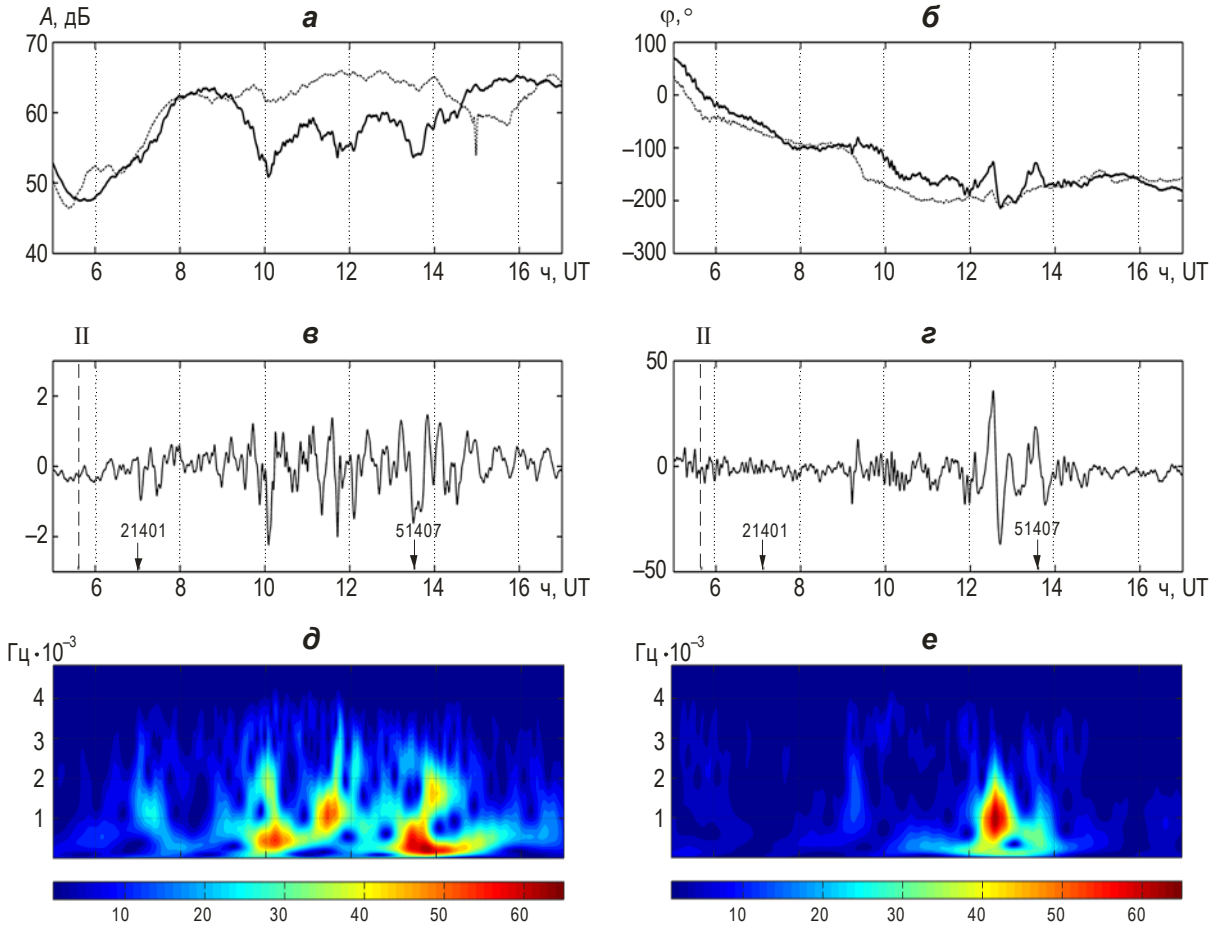


**Fig. 4.** (*a*) Amplitude and (*b*) phase of NPM signal recorded on 11.03.2011 at the MSR station (gray lines are the average monthly values of the considered parameter); (*c* and *d*) filtered signals. Vertical dashed line indicates the time of earthquake II that occurred on 11.03.2011; arrows is the time of tsunami wave arrival on buoys 21401 and 51407; and *e* and *f* are the wavelet spectra of filtered signals.

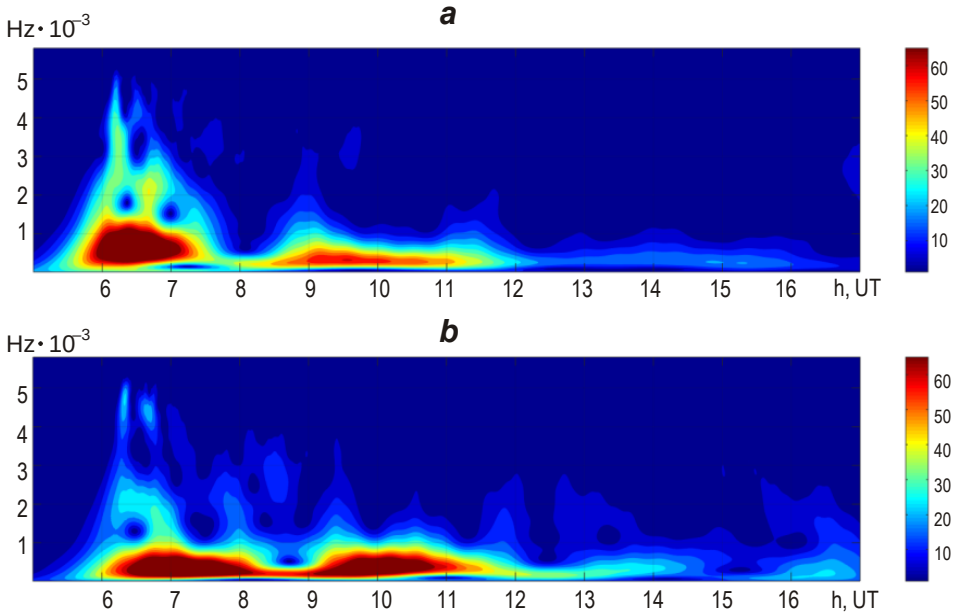


**Fig. 5.** Wavelet spectra of sea level fluctuations registered on 11.03.2011 from 5 to 17 UT by GPS stations on the buoys (*a*) 802 and (*b*) 807. Data from the Japanese Information Network NOWPHAS

threat to the entire Pacific coast including the Russian Far East. The propagation time of tsunami to Hawaii was about 14 h; it reached the coast of Kamchatka and the Kuril Islands in another 7 h. In Petropavlovsk-Kamchatsky, the first wave was recorded at 3:48 UT, in Severo-Kurilsk at 4:24 UT, and in Malo-Kurilsk at в 4:52 UT [*Shevchenko et al.,* 2012]. For the analysis of VLF signal variations after the earthquake, we used the path NPM–PTK (see Fig. 1). Path NPM–YSH was not included in the analysis because from 23.02.2010 till 01.03.2010 the signal at the YSH station was perturbed and after the transmitter was disconnected. Such long-term perturbations in VLF signal on the path NPM–YSH are possibly related to the series of earthquakes observed in this period in sensitivity zone of the path; the strongest among them occurred on 06.03.2010 with $M$=5.7.

Unlike the two tsunamis discussed above, in this case, the arrival of the first wave in the sensitivity zone of the path occurred in the daytime, that can't affect the behavior of VLF signal. However, the arrival of the second (reflected) wave on the next day during the local night caused strong perturbations in the signal that coincided with the moment of registration of the second tsunami wave by the DART station on the buoy 51407 located in Hawaii. This station, located at the beginning of the path NPM–PTK, registered the arrival of tsunami on 27.02.2010 approximately at 21:00 UT; station DART on the buoy 21416 located at the end of the path registered arrival of tsunami at 02:44 UT on 28.02.2010 [*Shevchenko et al.,* 2012]. During this entire period the path NPM–PTK was sunlit.

Figure 6 shows SWAN diagrams of sea level fluctuations records registered by DART receivers on the same buoys: record on the buoy 51407 is made within twenty-four hours from 1800 UT of 27.02.2010 till 18:00 UT of 28.02.2010, on the buoy 21416 starting from 00:00 UT of 28.02.2010.

Records on the buoy 51407 (see Fig. 6, *b*) clearly indicate two waves, the first one (main, the arrival time is 21:00 UT of 27.02.2010) has main frequency maximums with

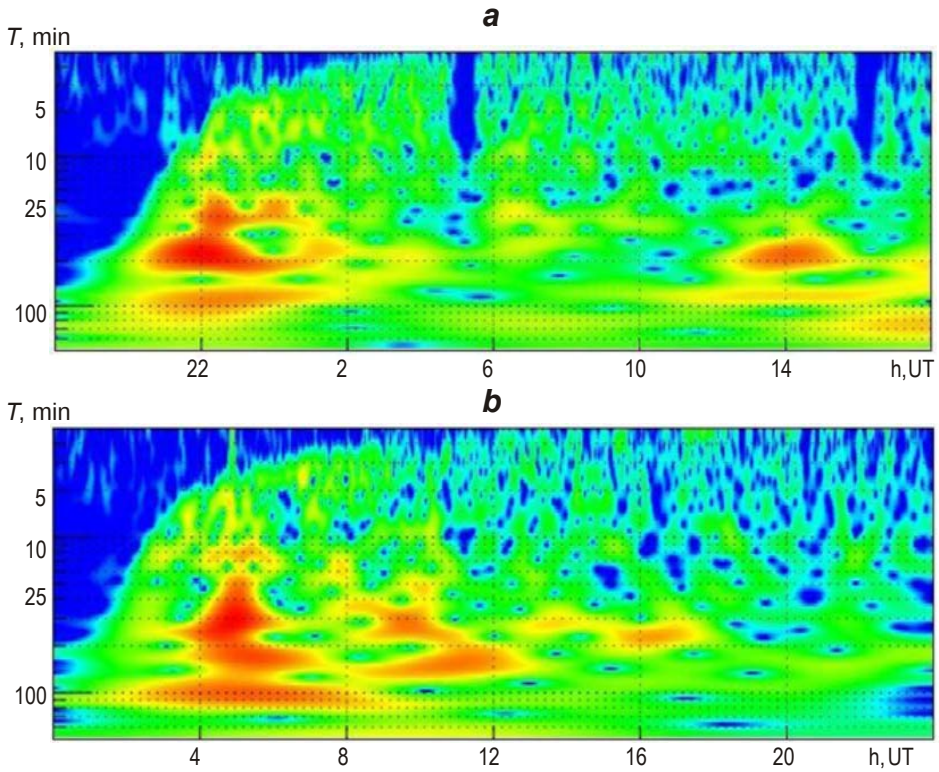


**Fig. 6.** SWAN diagrams of sea level fluctuations records registered by DART receivers on buoys (*a*) 51407 and (*b*) 21416. See explanations in the text

periods of 45-50 min and ~100 min, a weaker maximum at the periods of 20-25 min and minor fluctuations in high-frequency range (periods less than 10 min). Periods of second (reflected) wave (around 13:00 UT of 28.02.2010) cover the range of 30-60 min. Fluctuations of sea level registered on the buoy 21416 start around 03:00 UT and continue almost till the end of the day, whereas the increase in fluctuations with the main periods of 20 - 40 min is observed in the interval from 09:00 to 11:00 UT.

Wavelet-spectra of filtered signal of amplitude and phase of NPM signal recorded in Petropavlovsk-Kamchatsky during local night on 28.02.2010 are demonstrated in Fig.7. It can be seen that maximum of spectral amplitude is in the range of 0.3-2.5 MHz or 7-55 min. It is close to the periods registered on DART buoys, located at the beginning and end of propagation path of VLF signal, and also corresponds to the periods of internal gravity waves.

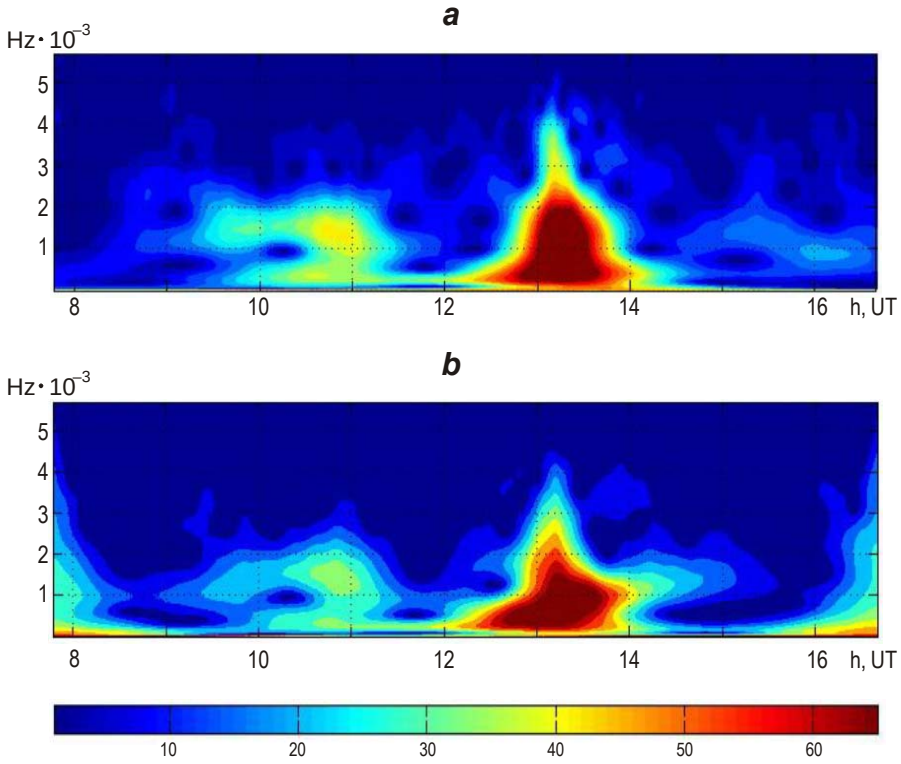


**Fig. 7.** Wavelet spectra of (*a*) amplitude and (*b*) phase of *NPM* signal recorded on 28.02.2010 in Petropavlovsk-Kamchatsky during local night. The frequency filtering was carried out in the band of 0.3-15 MHz. Comments see in the text

It should be noted that interaction of gravity waves with the lower ionosphere starts approximately at 9–11 UT coinciding with fluctuations increase, registered by receiver DART on the buoy 21416. Then after approximately the one-hour interval without perturbations (11:00–12:00 UT), the maximum perturbations started from 13:00 UT; at this time the second wave of tsunami reaches Hawaii.

## Conclusions

The results presented in the work showed that perturbations in the lower ionosphere caused by atmospheric internal gravity waves generated by tsunamis can be detected by sub-ionospheric VLF signals. It was revealed that frequency characteristics of perturbed VLF

signals recorded during tsunami propagation are compatible with frequency maximums of spectra in situ measurements of sea level fluctuations.

Detailed quantitative interpretation of observed effects in the terms of interaction of internal gravity waves with the lower ionosphere was made previously by *Rozhnoi et al.* [2012] and *Shalimov* [2013], who showed that atmospheric gravity waves generated by tsunami precede the tsunami waves according to the condition of radiation. This fact can be applied in the system of early warning of approaching tsunami

Thus, ionosphere monitoring by different methods including GPS observations, over-the-horizon radars, ionosphere glow registration, VLF signals propagation, etc., can be a useful tool for propagation monitoring and tsunami warning.

## Acknowledgements

The work was supported by the Russian Foundation for Basic Research (project nos. 14-05-00099, 13-05-92602_KO).

The authors are grateful to Professor M. Hayakawa from the University of electric communications, Chofu (Japan) and to assistant S. Mungov, National Geophysical Data Center at NOAA in Boulder (USA) for providing GPS and DART high resolution data about sea level fluctuations

## References

Artru J., Ducic V., Kanamori H., Lognonne P., and Murakami M. Ionospheric detection of gravity waves induced by tsunamis, *Geophys. J. Int*., 2005, vol.160, pp. 840–848, doi:10.1111/j.1365-246X.2005.02552.x.

Barr R., Jones D. Llanwyn, and Rodger C. J. ELF and VLF radio waves, *J. Atmos. Sol. Terr. Phys.,* 2000, vol.62, pp. 1689–1718.

Coïsson P., Occhipinti G., Lognonné P., and Rolland L. M. Tsunami signature in the ionosphere: the innovative role of OTH radar, *Radio Sci*., 2011, vol. 46. RS0D20, doi:10.1029/2010RS004603.

Galvan D.A., Komjathy A., Hickey M. P., and Mannucci A. J. The 2009 Samoa and 2010 Chile tsunamis as observed in the ionosphere using GPS total electron content, *J. Geophys. Res*., 2011, vol. 116. A06318, doi:10.1029/2010JA016204.

Hickey M. P., Schubert G., Walterscheid R. L. Atmospheric airglow fluctuations due to a tsunami-driven gravity wave disturbance, *J. Geophys. Res.,* 2010, vol. 115. A06308, doi:10.1029/2009JA014977.

Hines C. O. Gravity waves in the atmosphere, *Nature*, 1972, vol. 239, pp. 73– 78.

Komjathy A., Galvan D. A., Stephens P., Butala M. D., Akopian V., and Wilson B., Verkhoglyadova O., Mannucci A. J., Hickey M. Detecting ionospheric TEC perturbations caused by natural hazards using a global network of GPS receivers: The Tohoku case study, *Earth Planets Space*, 2012, vol. 64, N 12, pp. 1287–1294, doi:10.5047/eps.2012.08.003.

Makela J., Lognonne P., Hébert H., Gehrels T., Rolland L., Allgeyer S., Kherani A., Occhipinti G., Astafyeva E., Coïsson P., Loevenbruck A., Clévédé E., Kelley M. C., and Lamouroux J. Imaging and modeling the ionospheric airglow response over Hawaii to the tsunami generated by the Tohoku earthquake of 11 March 2011, *Gephys. Res. Lett*., 2011, vol. 38. L00G02, doi:10.1029/2011GL047860.

Najita K., Weaver P., and Yuen P. A tsunami warning system using an ionospheric technique, *Proc. IEEE*, 1974, vol. 62, no. 5, pp. 563–577.

Occhipinti G., Coïsson P., Makela J. J., Allgeyer S., Kherani A., Hébert H., and Lognonne P. Three-dimensional numerical modeling of tsunami-related internal gravity waves in the Hawaiian atmosphere, *Earth Planet. Sci.*, 2011, vol. 63, pp. 847–851, doi:10.5047/eps.2011.06.051.

Occhipinti G., Kherani A., and Lognonné P. Geomagnetic dependence of ionospheric disturbances induced by tsunamigenic internal gravity waves, *Geophys. J. Int*., 2008, vol. 173, N 3, pp. 753-765, doi: 10.1111/j.1365-246X. 2008.03760.x.

Occhipinti G., Lognonné P., Kherani E. A., and Hébert H. Three dimensional waveform modeling of ionospheric signature induced by the 2004 Sumatra tsunami, *Geophys. Res. Lett*., 2006, vol. 33. L20104, doi:10.1029/2006GL026865.

Peltier W. R. and Hines C. O. On the possible detection of tsunamis by a monitoring of the ionosphere, *J. Geophys. Res*., 1976, vol. 81, pp. 1995-2000, doi:10.1029/0JGREA000081000C12001995000001.

Rolland L. M., Occhipinti G., Lognonné P., and Loevenbruck A. Ionospheric gravity waves detected offshore Hawaii after tsunamis, *Geophys. Res. Lett*., 2010, vol. 37. L17101, doi:10.1029/2010GL044479.

Rozhnoi A., Shalimov S., Solovieva M., Levin B. W., Hayakawa M., and Walker S. N. Tsunami-induced phase and amplitude perturbations of subionospheric VLF signals, *J. Geophys. Res*., Space Physics 2012, vol. 117. A09313, doi:10.1029/2012JA017761.

Rozhnoi A., Shalimov S., Solovieva M., Levin B., Shevchenko G., Hayakawa M., Hobara Y., Walker S. N., and Fedun V. Detection of tsunami-driven phase and amplitude perturbations of subionospheric VLF signals following the 2010 Chile earthquake, *J. Geophys. Res. Space Physics*, 2014, vol. 119, 5012–5019, doi:10.1002/2014JA019766.

Shalimov S.L., Ionosphere above tsunami, *Nauchno-tehnicheskaya revolutsia* (Scientific-Technical Revolution), 2013, vol.92, no. 4, pp. 3-18.

Shevchenko Georgy, Ivelskaya Tatiana, Loskutov Artem, and Shishkin Alexander. The 2009 Samoan and 2010 Chilean Tsunamis Recorded on the Pacific Coast of Russia, *Pure Appl. Geophys*., 2012, vol. 170, N 9-10, pp. 1511-1527, doi 10.1007/s00024-012-0562-9.